1	Molecular genetic differentiation in earthworms inhabiting a heterogeneous Pb-polluted
2	landscape
3	
4	J. Andre ^{1,2} , R. A. King ¹ , S. R. Stürzenbaum ³ , P. Kille ¹ , M. E. Hodson ² and A. J.
5	Morgan ¹
6	
7	¹ Cardiff School of Biosciences, Cardiff University, Museum Avenue, Cardiff, CF10
8	3TL, UK.
9	
10	² Department of Soil Science, School of Human and Environmental Sciences,
11	University of Reading, Whiteknights, Reading, RG6 6DW, UK.
12	
13	³ King's College London, School of Biomedical & Health Sciences, Pharmaceutical
14	Sciences Division, London, SE1 9NH, UK.
15	
16	Corresponding Author: Dr Jane Andre, Cardiff School of Biosciences, Cardiff
17	University, Museum Avenue, Cardiff, CF10 3TL, UK. Email:Andrej@cardiff.ac.uk
18	
19	Abstract
20	
21	Landscapes blighted by industrial activity but which accommodate seemingly resistant
22	animal ecotypes provide an ideal opportunity to study evolution in action. We
23	investigated the phylogenetic structure and molecular adaptation of the metal
24	extremophile earthworm Lumbricus rubellus inhabiting a geochemically heterogeneous
25	Pb/Zn mine. These worms prodigiously accumulate Pb (c.1.5% total-body dry mass),

26	trafficking most to Ca/PO4-rich organelles in chloragocytes. Infrared
27	microspectroscopy (FTIR) of chloragocytes detected altered phosphate profiles in a
28	putative tolerant population. Moreover, bioinformatic analysis of <i>L. rubellus</i> EST ^{Pb}
29	libraries indicated that constituents of Ca-signalling and sequestration pathways were
30	aberrantly elevated. Sequencing a gene central to this pathway, sarco/endoplasmic
31	calcium ATPase (SERCA), revealed mutations clustered in the cytosolic domain that
32	correlated with site-specific Pb-tolerant genotypes. Our findings present a mechanism
33	that enables locally adapted earthworm populations to tolerate a novel habitat,
34	potentially contributing to genetic differentiation and eventual speciation. Additionally,
35	they indicate that extreme Pb tolerance mechanisms are evolutionary appropriations of
36	intrinsic Ca molecular machinery: Inorganic mimicry begets biomolecular adaptive
37	mechanisms.
38	
39	Capsule: Landscapes punctuated by polluted islands are inhabited by Pb-adapted
40	invertebrate extremophiles.
41	
42	Keywords: Calcium, lead, earthworms, phylogenetics, ecotoxicology
43	
44	
45	
46	
47	
48	
49	Introduction

50

51 Occupational and environmental exposures to Pb continue to cause serious human 52 health problems in developing and industrialised countries (Tong et al., 2000) and 53 diverse disruptive effects on both ecological processes (Rantalainen et al., 2006) and 54 wildlife (Chapman and Wang, 2000). Intriguingly some field populations (ecotypes) of 55 invertebrates have evolved resistance to metal stressors in their native habitats (Morgan 56 et al., 2007), with the earthworm *Lumbricus rubellus* representing an extreme example 57 of a complex organism that can manifest Pb tolerance in mine-associated soils 58 contaminated to a degree exceeding by an order of magnitude the exposure level that 59 severely compromises reproduction in spiked laboratory soils (Spurgeon et al., 1994). L. 60 *rubellus* is an acid-tolerant species inhabiting litter on soils ranging from pH 3.8 to 8.4 61 (Sims and Gerard, 1985), thereby indicating that this early pioneer of mine-associated 62 and industrial 'soils' may possess the genetic amplitude to become a locally-adapted 63 population with the inherent ability to cope with site-specific extremes in contaminant 64 availabilities. Although many terrestrial invertebrates reside in soils containing metal 65 levels that far exceed effect concentrations for key life-cycle traits (Morgan and 66 Morgan, 1990; Spurgeon and Hopkin, 1996) and despite being well documented in 67 plants, evidence for the heritability of adaptive traits and evolution of metal-resistant 68 ecotypes remain relatively sparse.

69

As sites elevated in inorganic pollutants illustrate both spatial and temporal
stochasticity, with geological features alongside ancient and recent industrial activities
providing an array of unique environments to which nature has adapted, cogent data sets
to investigate evolution in action are presented. The Cwmystwyth valley, Wales (UK) is

74 a disused Pb (galena, PbS) mine that is highly heterogeneous in nature comprising of 75 numerous micro-habitats that relate to soil metal content and pH. In combination with 76 the acquisition of Pb-adaptive traits in L. rubellus ecotypes, a unique model to study 77 earthworm phylogeography and, more specifically, whether metal contamination-78 associated stress and microsite heterogeneity have the potential to alter the genetic 79 structure of populations through adaptation and speciation is provided. The ancestors of 80 earthworms now resident at Cwmystwyth would have survived the major glaciations 81 and climatic instability of the Devensian period in one or more of the sheltered southern 82 refugia. With the onset of each stadial period and reformation of ice-sheets, retreating 83 bottlenecked populations would have experienced shrinkage, dissection and extinction, 84 whereas upon post-glacial expansion undergone adaptation and selection to new 85 environments (Hewitt, 2000). Repeated climatic oscillations and changes in habitat 86 range have therefore yielded increased species diversity through several genome 87 reorganisations, manifested today by the broad environmental conditions and 88 geographical ranges tolerated by L. rubellus. This includes the ability to colonise 89 heterogeneous and potentially stressful metal-polluted habitats such as are found at 90 Cwmystwyth.

91

Detrimental effects of Pb exposure arise from the ability of Pb to mimic other metals,
primarily Ca (Clarkson, 1993; Warren et al., 1998). Intracellular interactions between
Pb and Ca are well documented, with non-sequestered Pb metal ions shown to interact
and associate with proteins active in the calcium signalling pathway. This shared
chemical affinity between Pb and Ca lead us to hypothesise that the network of
mechanisms evolved to regulate the potentially lethal levels of intracellular free Ca²⁺ are

98 somehow implicated in the handling of its non-essential cationic analogue. Ordinarily 99 the main molecular resistance mechanisms underlying metal tolerance entails either 100 metal efflux pumps (Callaghan and Denny, 2002) or sequestration by one of three 101 classes of thiol-rich peptides, namely glutathione, phytochelatin and metallothionein 102 (Vatamaniuk et al., 2005; Janssens et al., 2007). However, neither of these generic 103 resistance mechanisms has been found to underpin Pb adaptations in earthworms or any 104 other organism. Instead, accumulated Pb is sequestered within calcium phosphate-rich 105 chloragosomes, unique organelles with certain lysosome-like properties that are located 106 in the chloragogenous tissue (Morgan and Morgan, 1989). It follows that specific 107 transport mechanisms must reside in vacuolar membranes for the uptake of metals and 108 accompanying anions, which provide the complexing negatively charged ion needed for 109 an insoluble precipitate to be formed. With this in mind, this study aimed to provide 110 insights into the functional mechanisms of Pb management and adaptation in 111 chronically exposed earthworm populations. This was achieved through global 112 transcriptomic analyses, targeted single loci experiments and in-situ biochemical 113 fingerprinting of the main metal sequestering organ of the earthworm. Combined with 114 characterising the entire site in terms of metal content and pH and, in parallel, 115 measuring population divergence from whole-genome and mtDNA loci, a sophisticated 116 means of studying earthworm speciation and evolution to ecological heterogeneity on a 117 micro-geographic scale is presented. 118

120

119

Materials and Methods

121 Portable XRF and pH mapping of the Cwmystwyth site. A portable XRF (NITON

122 XLiand, Thermo Scientific Inc) and GPS system (Garmin, Etrex Venture) were used in

123 order to create a Pb profile the Cwmystwyth valley, with a total of 97 measurements

taken. A series of 71 soil samples were also collected and the pH of each recorded. The

125 mapping software SURFER[©] was used to convert both the metal and pH data sets into a

series of 3D rendered surface maps, stacked alongside a base-map of the valley.

127

128 Mitochondrial and AFLP genotyping. Lumbricus rubellus earthworms were collected 129 by digging and hand-sorting. The animals were transported back to the laboratory in 130 their native soil and depurated as described in (Arnold and Hodson, 2007). Genomic DNA was extracted from $C1_{Pb^*}^{pH5}$ (n=27), $C2_{Pb^*}^{pH4}$ (n=33), $C3_{Pb^{***}}^{pH7}$ (n=32) and $C4_{Pb^*}^{pH6}$ (n=30) 131 132 earthworms using DNAzol reagent (Invitrogen Ltd., Paisley, UK.). DNA was also 133 isolated from *L. castaneus* and *L. eiseni*. Forward (5'-TAGCTCACTTAGATGCCA) 134 and reverse (5'-GTATGCGGATTTCTAATTGT) L. rubellus specific cytochrome 135 oxidase II (COII) primers were designed from mitochondrial sequences deposited in 136 LumbriBASE (www.earthworms.org). For each PCR reaction ~100ng DNA template 137 was amplified using 10pmole/µl forward and reverse primer, 10mM dNTP mix and 138 5U/µl Taq DNA polymerase buffered with 5X Mg-free Taq PCR amplification buffer 139 and supplemented with MgCl₂ (1.5mM). The reaction was denatured at 95°C for 10 140 minutes and then cycled 35 times at 95°C for 30 seconds, 30 seconds at the required 141 primer annealing temperature and 72° for 1 minute. This was followed by a 10 minute 142 final extension at 70°C. The amplicon (469bp) was resolved by electrophoresis in 1X 143 TAE buffer at 120V for approximately 30 minutes in a Pharmacia GNA-100 tank. 144 Nucleic acid bands were then visualised on a UV gel documentation system. Prior to

145	sequencing PCR clean-ups were performed using Exo-SAP-IT (Amersham Pharmacia,
146	UK) reagents. Exonuclease 1 (0.25 μ l) and Shrimp Alkaline Phosphatase (0.5 μ l) were
147	mixed with the PCR product (10µl) and incubated at 37°C for 45 minutes followed by
148	80°C for 15 minutes. DNA was sequenced using ABI PRISM [®] BigDye v3.1 Terminator
149	Sequencing technology (Applied Biosystems, Foster City, USA) on the ABI $PRISM^{$ ®}
150	3100 DNA Sequencer run by the Cardiff University Molecular Biology Support Unit.
151	Raw sequence traces were confirmed using Finch TV before being imported into Mega
152	v3.1 (Kumar et al., 2004) for alignment and tree construction. The distance-based
153	neighbour joining (NJ) algorithm (Saitou and Nei, 1987), using p-distances, was used to
154	estimate tree topology and calculate branch lengths. Relationships between phylogenetic
155	haplotypes were determined by maximum parsimony (MP), maximum likelihood (ML)
156	and Bayesian methods using PAUP v3.1 and MRBAYES respectively (Huelsenbeck
157	and Crandall, 1997; Huelsenbeck and Ronquist, 2001), MRMODELTEST v2.2
158	(Nylander, 2004) and the Akaike Information Criterion (AIC) were used to select the
159	optimum model (HKY+G) of sequence evolution that best fitted the data (base
160	frequencies of A=0.3638, C=0.2244, G=0.1277, T=0.2842 and T-ratio=3.5050 and
161	Gamma distribution parameter= 0.2005). Node support for MP and ML analyses was
162	determined using a non-parametric bootstrap, with 500 and 1000 replicates respectively
163	(Holmes, 2003). For the analysis 3x106 generations were run, with one tree retained
164	every 300th generation and the first 2500 trees discarded as burn-in. Genetic distances
165	were calculated using p-distance in Mega and median-joining networks were drawn
166	using NETWORK and dnasp4.
167	

168	AFLP analysis was adapted from (Ajmone-Marsan et al., 1997) with approximately
169	200ng of genomic DNA extracted from $C1_{Pb^*}^{pH5}$ (n=24), $C2_{Pb^*}^{pH4}$ (n=30), $C3_{Pb^{***}}^{pH7}$ (n=23) and
170	$C4_{Pb^*}^{pH6}$ (n=18) individuals. Pre-selective EcoR1 (GACTGCGTACCAATTCA) and Taq1
171	(GACTGCGTACCAATTCC) primers were used and for the selective amplifications
172	two primer combinations (E32 (5'-GACTGCGTACCAATTCAAC-3') /T32 (5'-
173	GATGAGTCCTGACCGAAAC-3') and E32/T38 5'-GATGAGTCCTGAC CGAACT-
174	3') were employed. Reactions were run by the Cardiff University Molecular Biology
175	Support Unit and analysed on an Applied Biosystems 3130x1 fragment analyser. Bands
176	between 70 and 325 base pairs (bp) and with a minimum peak height of 70 units were
177	scored using GeneMapper analysis software. Microsoft Access, Excel and the Excel
178	macro GenAlEx6 were used to create a cumulative table of all loci from each individual
179	and transform the data into a binary form. Principal coordinates (PCO) analysis and
180	phylogenetic tree construction, supported by bootstrap analysis (1000 replicates), was
181	performed using the neighbour joining algorithm (based upon the Nei's distance) to in
182	PAUP v4.0b10 to estimate tree topology and calculate branch length. The software
183	Structure v2.2 was used to delineate clusters of individuals on a multi-locus, genotype
184	basis using a Bayesian algorithm. The number of inferred populations ran from 1 to 5,
185	with 8 replicate runs, a burn-in of 75 000 cycles followed by 300 000 for data
186	collection. L(K), the modal choice criterion, is calculated in Structure and the true
187	number of populations (K) can be deferred from its maximal value. ΔK , the rate of
188	change in the log probability of data between successive K-values, provides a visual
189	means to easily identify the number of clusters in a sample of individuals (Evanno et al.,
190	2005).

EST libraries and informatics. Upon sampling $C3_{Pb^{***}}^{pH7}$ (n=5) earthworms were 192 193 immediately immersed and maintained in liquid nitrogen and stored at -80°C until 194 required. R1 (n=5) earthworms were transported back to the laboratory in their native soil and individuals exposed to 500, 750, 1250, 1750 and 2250 mg/kg^{-1} Pb in the form 195 196 of Pb(NO₃)₂ spiked Kettering loam soil and maintained at a WHC of 75% for three 197 weeks at 15°C. Spiked soil was left to equilibrate for three days prior to earthworm 198 addition. Following exposure, earthworms were snap-frozen in liquid nitrogen and 199 stored at -80°C. Earthworm total RNA (~1.25mg) was extracted using the TRI-reagent 200 method (Sigma-Aldrich, UK) and mRNA isolated using an mRNA Purification Kit 201 (Amersham, UK). cDNA libraries were constructed using the pBluescript® II XR 202 cDNA Library Construction Kit (Stratagene Europe, Amsterdam, The Netherlands). 203 PCR was used to screen the libraries and quantify insert size. Each PCR contained 5µl 204 neat culture, 10X Triton free PCR Buffer (10µl), MgCl2 (0.25µl, 1mM), universal 205 M13F and M13R primers (0.2µl, 10mM), dATP, dCTP, dTTP, dGTP (0.2µl, 100mM) 206 and Taq polymerase (0.16µl, 50U/ml) in a 95µl reaction. The reaction was denatured at 207 95°C for 10 minutes and then cycled 35 times at 95°C for 30 seconds, 30 seconds at the 208 primer annealing temperature of 56°C and 72° for 1 minute. This was followed by a 10 minute final extension at 70°C. Products were resolved by electrophoresis using E-Gel[®] 209 210 technology (Invitrogen Ltd., Paisley, UK) and associated editing software. High quality clones were cherry-picked using the MultiPROBE[®] II HT EX liquid handling system 211 (PerkinElmer, Bucks., UK) and associated WinPrep[®] software. The composite plate 212 products were purified using Montage[®] Multiscreen PCRµ96 cleanup plates by vacuum 213 214 filtration and the DNA was resuspended in sterile water (30µl). Sequencing reactions 215 were completed by the SBSSS facility at Edinburgh University and sequences named

216 according to the NERC Environmental Genomics scheme to allow for bioinformatics 217 analysis. The raw trace chromatograms from the sequencing reaction were processed 218 using trace2dbEST (Sturzenbaum et al., 2003) which contains a base calling component 219 (phred) and a sequence trimming component (cross_match). This software produces 220 good quality EST sequences, formatted for submitting to NCBI dbEST 221 (http://www.ncbi.nlm.nih.gov/dbEST). The EST sequences were clustered using 222 CLOBB (Sturzenbaum, et al., 2003) to derive a consensus putative gene sequence 223 contig and then processed by the software package PartiGene (Sturzenbaum, et al., 224 2003) (http://www.nematodes.org/PartiGene). Cluster information can be retrieved by 225 LumbriBASE (http://www.earthworms.org) through simple text queries, identification 226 of sequence similarity and library specific searches. The biological process and 227 molecular function of gene sequences were described by defining their Gene Ontology 228 (GO) classification using blast2go (http://www.blast2GO.de).

229

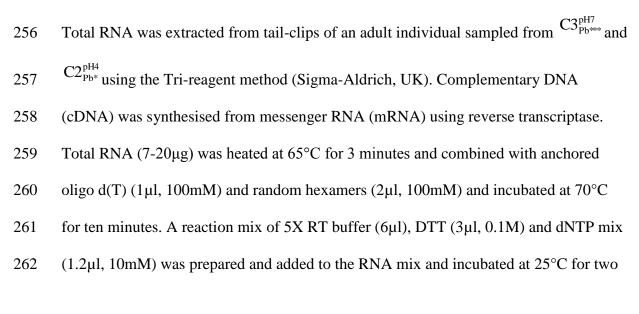
230 <u>Fourier-transform Infrared Spectroscopy</u>. Soil and adult (fully clitellate) *L. rubellus*

earthworms were collected from $C2_{Pb^*}^{pH4}$ and $C3_{Pb^{***}}^{pH7}$ and the posterior segments 231 232 immediately excised and quench-frozen in liquid nitrogen. The frozen tissue was 233 transported to the laboratory under liquid nitrogen and stored at -20°C until required. 234 Tissues were mounted in CryoEmbed and sectioned longitudinally at a nominal 235 thickness of 50µm in a Bright cryostat. Sections were mounted on Kevley slides and air-236 dried overnight in the cold chamber of the cryostat. Infra-red spectra were collected in 237 transmission mode from station 11.1 at the CLRC Daresbury Synchrotron Radiation 238 Source. The chloragogenous tissue was visually identified and each section imaged and

analysed, with five spectra from five different regions of the tissue (i.e. x25 spectra perindividual earthworm) collected.

241

242 SERCA. Plasmid preparations of individual LumbriBASE clones (Genbank accession numbers CF416761 and CO048347) were prepared using a Wizard[®] Plus SV Miniprep 243 244 kit (Promega Ltd., Southampton, UK). Preparations were sequenced in their entirety by 245 "walking" along the gene, after each step re-designing a specific reverse primer to 246 complement the universal M13 forward. Primers were designed using the software Primer3 (Rozen and Skaletsky, 2000) and Oligo[®] (MBI Inc, USA) and sequencing 247 248 performed as described above. These full-length library sequences were used to design 249 L. rubellus specific SERCA primers in order to amplify the gene transcribed in 250 individuals of each genealogical lineage. Reactions were denatured at 95°C for 10 251 minutes and then cycled 35 times at 95°C for 30 seconds, 30 seconds at the required 252 primer annealing temperature and 72° for 1 minute. This was followed by a 10 minute 253 final extension at 72°C. DNA was sequenced as described above by the Cardiff 254 University Molecular Biology Support Unit. 255



263 minutes. Superscript (1µl) was added and the reaction incubated at 42°C for 3 hours. A 264 series of three PCR reactions were optimised and performed in order to obtain the full-265 length SERCA sequence of each individual; between sequenced sections of the gene 266 there was a large overlap to ensure the same SERCA isoform was being amplified in 267 each instance. PCRs were performed as described above. Reactions that yielded 268 products >2000 bp were modified. For these reactions DNA (~100ng) template was 269 amplified using 10µM forward and reverse primer, 25mM dNTP mix and 1µl 270 Herculase® II Fusion DNA Polymerase buffered with 5X Herculase® II PCR reaction 271 buffer (Stratagene Europe, Amsterdam, The Netherlands). Each reaction was 272 supplemented with an optimised quantity of MgCl₂ (25mM). The reaction was 273 denatured at 95°C for 10 minutes and then cycled 35 times at 95°C for 20 seconds, 20 274 seconds at the required primer annealing temperature and 68° for 4 minutes. This was 275 followed by a 4 minute final extension at 68°C. Protein sequences were aligned using 276 bioinformatic software tool Mega v3.1 (Kumar, et al., 2004) and modelled using 277 SWISS-MODEL (http://swissmodel.expasy.org//SWISS MODEL.html), Swiss-278 PdbViewer and Pymol.

279

Total RNA was extracted from nine, previously genotyped (mtDNA) adult individuals sampled from Cl^{pH5}_{Pb*}, C2^{pH4}_{Pb*}, C3^{pH7}_{Pb***} and C4^{pH6}_{Pb*}. This was followed by cDNA synthesis, as described above. A PCR was designed to enable easy identification by gel electrophoresis of the expressed isoform, with a combination of three primers used in each reaction (F1 5'-CTGGCCGGAATTCGTGTTATC-3', F2 5'-ATACTCTTCG CTGTCTTGCGT-3', R1 5'-CCGCTGGCTCTTCTTCCG-3'). The two forward primers were designed so that each one isolated one of the two isoforms. The resulting products were of different sizes to enable simple identification on an agarose gel followingresolution by electrophoresis.

289

290 Results and Discussion

291

292 The 'field laboratory': the metalliferous site and its resident earthworms. Mine sites are 293 notoriously heterogeneous in geochemical nature. Mineral (galena, PbS) extraction from 294 the Cwmystwyth Mine stopped in 1921. Today, the contaminated surface spoils are 295 situated on base-poor underlying geology, punctuated by calcareous 'islands' around 296 derelict buildings (Figure 1). In the decades since its abandonment, the spatially 297 chequered and hostile site has developed micro-habitats colonised by a limited variety 298 of naturally occurring plants and invertebrates. Thus, it serves as an ideal evolutionary 299 field laboratory. L. rubellus was sampled from four sites across the mine: Cl_{Pb*}^{pH5} , $C2_{Pb*}^{pH4}$, $C3_{Pb***}^{pH7}$, and $C4_{Pb*}^{pH6}$ (the number of asterisks denotes the level of 300 301 contamination as classified by the Kelly index (ICRCL 59/83): * contaminated (1000-302 2000ppm), ** heavily contaminated (2000-10 000ppm) and *** unusually heavily 303 contaminated (>10 000ppm) (Figure 1). Population divergence was measured using 304 amplified fragment length polymorphism (AFLP) analysis and mitochondrial 305 cytochrome oxidase II (mtDNA COII) gene sequence data of individuals split between 306 the four sites. Two distinct lineages, differentiated at both the mitochondrial and nuclear 307 level, were revealed with a mean inter-lineage mtDNA sequence divergence of 308 approximately 13%, indicative of a cryptic species complex (Figures 2A and B). Moreover, from the distinct clustering of $C3_{Pb^{****}}^{Ph^{7}}$ individuals a true genetic archipelago 309 310 is inferred that can be related to the calcareous, circum-neutral (pH6.5) and heavily

311 polluted nature of this island in an otherwise acidic, moderately polluted environment.
312 Such cryptic complexes are typical in taxa that thrive in specialised environments and it
313 perhaps explains why islands of anthropogenic contamination result in the loss or
314 "erosion" of genetic diversity. Potential adaptive and sympatric speciation processes
315 may be occurring, with the concurrent, contaminant-driven acquisition of adaptive gene
316 complexes in response to the unique nature of the site.

317

318 As phylogenetic population structure is shaped by ongoing processes of genetic drift 319 and gene flow, combined with past historical events, unravelling the L. rubellus species 320 complex requires inferences on both the structure of the phylogeny and demographic 321 tendencies. Accurately inferring the population-level dynamics of evolutionary 322 mechanisms that involve adaptive, and also sympatric, speciation is complex, especially 323 as the process is not clearly defined and involves both temporal and spatial 324 stochasticity. The timeline of divergence leading to sustained differentiation is neither 325 rapid nor definable and, due to the combined effects of gene flow and selection of 326 adaptively important genes, the genomes of incompletely isolated populations will 327 contain an assortment of variable and undifferentiated regions (Supporting data). 328 Fluctuations in the global climate have led to major ice ages during the Quaternary 329 period, with the Pleistocene epoch (1 808 000 to 11 500 before present (BP)) covering 330 the most recent period of repeated glaciations. Glaciation evidence can be related to the 331 profile of mtDNA haplotypes in both lineage A and B, the shape of the corresponding 332 mismatch distributions (Figures 2C and D), and estimated time since population 333 expansion. Lineage A comprises nine haplotypes that contain two or more individuals. 334 This, combined with a ragged multimodal mismatch distribution, is suggestive of a

335 stationary population that has undergone multiple introductions and bottleneck episodes 336 (Harpending, 1994). Additionally, from the parameters Tau and date of growth in 337 mutational units, expansion is estimated to have occurred approximately 250 000 years 338 BP (assuming one generation per year) and may have corresponded with a non-glacial 339 environment such as the Hoxnian interstadial (~250 000 BP) (Brown, 1979) (Figure 340 2E). In contrast, lineage B consists of three haplotypes that contain two or more 341 individuals, and displays a unimodal mismatch distribution, and a post-glacial 342 population expansion time of approximately 17 000 years BP was calculated. This 343 combined evidence suggests that the population experienced a single burst of growth 344 and expanded after the height of the last glaciation period (~25 000 BP) with adaptation 345 or selection occurring in response to the warmer climate experienced towards the end of 346 the Devensian glaciation and onset of the Windermere interstadial (Brown, 1979; 347 Harpending, 1994).

348

349 'In-situ' biochemical fingerprinting and EST libraries from Pb-mine and laboratory

350 <u>exposed naïve worms.</u> These field earthworm populations prodigiously accumulate up

to 1.5% of total body dry mass Pb (Morgan, 2001), with Ca/PO₄-rich earthworm

352 chloragocyte cells constituting the main metal sequestering organ (Cotter-Howells et al.,

353 2005). Fourier transform infrared (FT-IR) microspectroscopy on a high energy

354 synchrotron source was used to determine the chemical composition of cryo-sectioned

355 chloragocytes in earthworms belonging to each lineage at the two heavily polluted,

albeit one acidic ($^{C2_{Pb^*}^{pH4}}$) and one calcareous ($^{C3_{Pb^{***}}^{pH7}}$), mine sites. The chlorogogenous tissue was found to have a distinctive FTIR spectrum (Supporting data) and site-specific disparities in the composition of chlorogogenous tissue (in the 1100cm⁻³ region of the

359 spectrum) were apparent, which correlated with phosphorous-containing functional 360 groups (Figure 3A and B). As the earthworm chloragocyte is thought to be involved in 361 haem biosynthesis (Jamieson and Molyneux, 1981), a conserved pathway that is 362 inhibited by Pb at several junctures (Warren, et al., 1998), Pb trafficking into and across 363 earthworm chloragocytes must be tightly regulated in these animals that are 364 continuously exposed to high concentrations of metal in their native environments and 365 whose strategy for dealing with it involves intracellular accumulative immobilization. 366 Indeed, inferences on the mechanisms of adaptive evolution to environmental 367 heterogeneity require not only abstract genotype- to phenotype associations but more 368 meaningful molecular genetic interpretations regarding the nature of induced 369 phenotypic variation. The transcriptomic profile of an organism provides a snapshot of 370 gene expression to provide information regarding developmental stage, life-history or 371 responses in relation to particular environmental stressors. EST libraries are also the 372 substrate for comparative genomic studies, through investigating differential expression 373 between cDNA populations. Two libraries were constructed from earthworm populations with contrasting histories of Pb exposure; C3^{pH7}_{Pb***} earthworms, chronically 374 375 exposed in the field, and earthworms sampled from a clean reference site, R1, acutely 376 exposed to lead in the form of $Pb(NO_3)_2$ under laboratory conditions. In combination 377 with the plethora of EST cluster information already available in LumbriBASE 378 (www.earthworms.org), originating from control (adult, head-enriched), life-stage (late 379 cocoon, juvenile) and other exposure (Cu, Cd, fluoranthene, atrazine) libraries, a metal 380 tolerant genotype may be related to phenotype and the functional systems that underlie 381 lead handling within these earthworm populations defined. Both libraries comprised 382 high quality sequences with an average length of between 500 and 600 base pairs. This

383 ensured the maximum numbers of sequences were annotated to enable accurate 384 downstream analysis and interpretation using the software LumbriBASE, Blast2GO and 385 associated KEGG resource, which generates pathway maps that highlight gene ontology 386 relationships between annotated sequences. Of interest was the significant number of $C3_{Pb^{***}}^{pH7}$ gene products (when compared to other libraries) associated with intracellular 387 388 Ca²⁺ sensing (Calmodulin, Troponin C) and buffering (Sarcoplasmic calcium binding 389 protein (SCP), Parvalbumin) (Gao et al., 2006; Ishida and Vogel, 2006). Both sets of 390 proteins belong to the EF-hand super-family of proteins implicated in calcium binding 391 and central to the Ca-signalling pathway. These observations indicate that components 392 of the Ca signalling pathway are central to Pb sequestration within chloragocytes which, 393 in turn, may be associated with adjustments in the metabolism of their common 394 complexing PO_4^- anion. This yields a number of candidate loci that may contribute to a 395 Pb-tolerance phenotype by modifying molecules involved in the cellular physiology of an essential cation (Ca^{2+}) to accommodate its non-essential cationic mimic (Pb^{2+}). 396

397

398 <u>Sarcoplasmic/ endoplasmic reticulum calcium ATPase (SERCA)</u>.

399 Sarcoplasmic/endoplasmic reticulum calcium ATPase (SERCA) is a central transport 400 carrier protein of the Ca signalling pathway that resides in membranes of intracellular 401 storage sites for the uptake of excess Ca and, conceivably, Pb (Tsien et al., 1987). Three 402 isoforms have been described in vertebrates (MacLennan et al., 1985; Campbell et al., 403 1991; Vilsen and Andersen, 1992) and one in invertebrates (Palmero and Sastre, 1989; 404 Escalante and Sastre, 1994; Shi et al., 1998a; b), fungi (Ghislain et al., 1990) and plants 405 (Wimmers et al., 1992). All isoforms are similar in structure and have a 75-85% 406 identical amino acid sequence (Toyofuku et al., 1992). Despite the identification of

407 several vertebrate isoforms, L. rubellus is the first invertebrate found to harbour 408 multiple SERCA proteins. Two structurally different forms were identified in 409 populations, sampled from different field sites, and expression was found to be co-410 incident with the mitochondrial lineage marker (COII), even where nuclear 411 hybridisation was observed (Figure 4A and B). Their structure differed in amino acids 412 located in the cytosolic nucleotide-binding domain (the flap) of the protein, a region 413 thought to have a critical role in determining calcium affinity and turnover (Figure 4C). 414 This observation indicates that not only are the intracellular trans-membrane Ca and Pb 415 pathways confluent at the molecular (SERCA) level and are associated with adjustments 416 in the metabolism of their common complexing PO_4^- anion, but the entire machinery is 417 demonstrably genotype-specific (Figure 4C). It is important to point out, however, that 418 whist the SERCA molecule is an important connector between the vulnerable cytosol 419 and the intra-vesicular depository of immobilized Pb, other components of the Ca 420 pathway warrant study to determine whether they are structurally or functionally 421 modified.

422

423 Conclusion

424

Findings presented here demonstrate that tolerance in earthworms with a protracted history of Pb exposure is not merely an expression of genetic divergence, rather that field populations may evolve Pb-adaptation traits by modifying molecular regulators of Ca physiology. Whilst adaptive changes in enzyme structure are, for good reason, less probable than changes in the promoters that regulate enzyme expression (Crawford et al., 1999b; a), they are clearly not molecular traits that can be ignored, as the similarity

431	in the ionic radii of Ca^{2+} (1.00Å) and Pb^{2+} (1,19Å) (Bridges and Zalups, 2005) may, for
432	example, facilitate structural mutations. Together, these observations describe a
433	molecular mechanism for Pb resistance in earthworms that may underpin their
434	phylogenetic differentiation within fairly discrete microhabitats across the study site.
435	Furthermore, the concept serves as a paradigm for invertebrates generally because the
436	ability for incorporating Pb into 'calcospherites' is ubiquitous, demonstrating that
437	evolution innovates by modifying existing structures or pathways.
438	
439	Acknowledgments
440	This work was performed during the tenure of a Natural Environmental Research
441	Council studentship (JA) registered at Reading University (NER/S/A/2004/12418). The
442	FTIR was performed at the Daresbury Synchrotron, Station 11.1, managed by Dr F.
443	Bahrami (CCLRC beamtime award 45211). We would like to thank Dr Peter Brabham
444	(School of Earth, Ocean and Planetary Sciences, Cardiff University) for his geomapping
445	support.
446	
447	References
448	Ajmone-Marsan, P., Valentini, A., Cassandro, M., Vecchiotti-Antaldi, G., Bertoni, G.,
449	Kuiper, M., 1997. AFLP markers for DNA fingerprinting in cattle. Animal Genetics 28,
450	418-426.
451	Arnold, R.E., Hodson, M.E., 2007. Effect of time and mode of depuration on tissue
452	copper concentrations of the earthworms Eisenia andrei, Lumbricus rubellus and

Lumbricus terrestris. Environmental Pollution 148, 21-30.

- 454 Bridges, C.C., Zalups, R.K., 2005. Molecular and ionic mimicry and the transport of
- 455 toxic metals. Toxicology and Applied Pharmacology 204, 274-308.
- 456 Brown, E.H., 1979. The Shape of Britain. Transactions of the Institute of British
- 457 Geographers, 449–462.
- 458 Callaghan, A., Denny, N., 2002. Evidence for an Interaction between p-Glycoprotein
- 459 and Cadmium Toxicity in Cadmium-Resistant and-Susceptible Strains of Drosophila
- 460 melanogaster. Ecotoxicology and Environmental Safety 52, 211-213.
- 461 Campbell, A.M., Kessler, P.D., Sagara, Y., Inesi, G., Fambrough, D.M., 1991.
- 462 Nucleotide sequences of avian cardiac and brain SR/ER Ca⁽²⁺⁾-ATPases and functional
- 463 comparisons with fast twitch $Ca^{(2+)}$ -ATPase. Calcium affinities and inhibitor effects.
- 464 Journal of Biological Chemistry 266, 16050-16055.
- 465 Chapman, P.M., Wang, F., 2000. Issues in Ecological Risk Assessment of Inorganic
- 466 Metals and Metalloids. Human and Ecological Risk Assessment 6, 965-988.
- 467 Clarkson, T.W., 1993. Molecular and Ionic Mimicry of Toxic Metals. Annual Review
- 468 of Pharmacology and Toxicology 33, 545-571.
- 469 Cotter-Howells, J., Charnock, J.M., Winters, C., Kille, P., Fry, J.C., Morgan, A.J., 2005.
- 470 Metal compartmentation and speciation in a soil sentinel: The earthworm, *Dendrodrilus*
- 471 *rubidus*. Environmental Science & Technology 39, 7731-7740.
- 472 Crawford, D.L., Segal, J.A., Barnett, J.L., 1999a. Evolutionary analysis of TATA-less
- 473 proximal promoter function. Mol Biol Evol 16, 194-207.
- 474 Crawford, D.L., Segal, J.A., Barnett, J.L., 1999b. Evolutionary analysis of TATA-less
- 475 proximal promoter function. Molecular Biology and Evolution 16, 194-207.
- 476 Escalante, R., Sastre, L., 1994. Structure of Artemia franciscana sarco/endoplasmic
- 477 reticulum Ca-ATPase gene. Journal of Biological Chemistry 269, 13005-13012.

478	Evanno, G., Regnaut, S., Goudet, J., 2005. Detecting the number of clusters of
479	individuals using the software STRUCTURE: a simulation study. Molecular Ecology
480	14, 2611-2620.

- 481 Gao, Y., Gillen, C.M., Wheatly, M.G., 2006. Molecular characterization of the
- 482 sarcoplasmic calcium-binding protein (SCP) from crayfish Procambarus clarkii.
- 483 Comparative Biochemistry and Physiology Part B Biochemistry & Molecular Biology
 484 144, 478-487.
- 485 Ghislain, M., Goffeau, A., Halachmi, D., Eilam, Y., 1990. Calcium homeostasis and
- 486 transport are affected by disruption of cta3, a novel gene encoding $Ca^{2(+)}$ -ATPase in
- 487 Schizosaccharomyces pombe. Journal of Biological Chemistry 265, 18400-18407.
- 488 Harpending, H.C., 1994. Signature of Ancient Population-Growth in a Low-Resolution
- 489 Mitochondrial-DNA Mismatch Distribution. Human Biology 66, 591-600.
- 490 Hewitt, G., 2000. The genetic legacy of the Quaternary ice ages. Nature 405, 907-913.
- 491 Holmes, S., 2003. Bootstrapping phylogenetic trees: Theory and methods. Statistical
- 492 Science 18, 241-255.
- 493 Huelsenbeck, J.P., Crandall, K.A., 1997. Phylogeny estimation and hypothesis testing
- 494 using maximum likelihood. Annual Review of Ecology and Systematics 28, 437-466.
- 495 Huelsenbeck, J.P., Ronquist, F., 2001. MRBAYES: Bayesian inference of phylogenetic
- 496 trees. Bioinformatics 17, 754-755.
- 497 Ishida, H., Vogel, H.J., 2006. Protein-peptide interaction studies demonstrate the
- 498 versatility of calmodulin target protein binding. Protein and Peptide Letters 13, 455-
- 499 465.
- 500 Jamieson, B.G.M., Molyneux, B.G., 1981. The Ultrastructure of the Oligochaeta.
- 501 Academic Press.

- 502 Janssens, T.K.S., Marien, J., Cenijn, P., Legler, J., van Straalen, N.M., Roelofs, D.,
- 503 2007. Recombinational micro-evolution of functionally different metallothionein
- 504 promoter alleles from Orchesella cincta. BMC Evolutionary Biology 7, 88.
- 505 Kumar, S., Tamura, K., Nei, M., 2004. MEGA3: Integrated software for Molecular
- 506 Evolutionary Genetics Analysis and sequence alignment. Briefings in Bioinformatics 5,
- 507 150-163.
- 508 MacLennan, D.H., Brandl, C.J., Korczak, B., Green, N.M., 1985. Amino-acid sequence
- 509 of a $Ca^{2+}Mg^{2+}$ -dependent ATPase from rabbit muscle sarcoplasmic reticulum, deduced
- 510 from its complementary DNA sequence. Nature 316, 696-700.
- 511 Morgan, A.J., Kille, P., Sturzenbaum, S.R., 2007. Microevolution and ecotoxicology of
- 512 metals in invertebrates. Environmental Science & Technology 41, 1085-1096.
- 513 Morgan, J.E., Morgan, A.J., 1989. The Effect of Lead Incorporation on the Elemental
- 514 Composition of Earthworm (Annelida, Oligochaeta) Chloragosome Granules.
- 515 Histochemistry 92, 237-241.
- 516 Morgan, J.E., Morgan, A.J., 1990. The distribution of cadmium, copper, lead, zinc and
- 517 calcium in the tissues of the earthworm *Lumbricus rubellus* sampled from one
- 518 uncontaminated and four polluted soils. Oecologia 84, 559-566.
- 519 Morgan, J.E., Richards, S. P., Morgan, A. J., 2001. Stable strontium accumulation by
- 520 earthworms; a paradigm for radiostrntium interactions with its cationic analogue,
- 521 calcium. Environmental Toxicology and Chemistry 20, 1236-1243.
- 522 Nylander, J.A.A., 2004. MrModeltest v2. Program distributed by the author.
- 523 Evolutionary Biology Centre, Uppsala University.

- 524 Palmero, I., Sastre, L., 1989. Complementary DNA cloning of a protein highly
- 525 homologous to mammalian sarcoplasmic reticulum Ca-ATPase from the crustacean
- 526 Artemia. Journal of Molecular Biology 210, 737-748.
- 527 Rantalainen, M.L., Torkkeli, M., Strommer, R., Setala, H., 2006. Lead contamination of
- an old shooting range affecting the local ecosystem--A case study with a holistic
- 529 approach. Science of the Total Environment 369, 99-108.
- 530 Rozen, S., Skaletsky, H., 2000. Primer3 on the WWW for general users and for
- 531 biologist programmers. Methods in Molecular Biology 132, 365-386.
- 532 Saitou, N., Nei, M., 1987. The Neighbor-Joining Method a New Method for
- 533 Reconstructing Phylogenetic Trees. Molecular Biology and Evolution 4, 406-425.
- 534 Shi, X., Chen, M., Pe, H., Hardwicke, P.M.D., 1998a. Amino acid sequence of a Ca 2-
- transporting ATPase from the sarcoplasmic reticulum of the cross-striated part of the
- adductor muscle of the deep sea scallop: comparison to serca enzymes of other animals.
- 537 Comparative Biochemistry and Physiology Part B Biochemistry & Molecular Biology
- 538 120, 359-374.
- 539 Shi, X., Chen, M., Pe, H., Hardwicke, P.M.D., 1998b. Amino acid sequence of a Ca 2-
- 540 transporting ATPase from the sarcoplasmic reticulum of the cross-striated part of the
- adductor muscle of the deep sea scallop: comparison to serca enzymes of other animals.
- 542 Comparative Biochemistry and Physiology Part B 120, 359-374.
- 543 Sims, R.W., Gerard, B.M., 1985. Earthworms: keys and notes for the identification and
 544 study of the species. Brill Archive.
- 545 Spurgeon, D.J., Hopkin, S.P., 1996. Effects of metal-contaminated soils on the growth
- 546 and, sexual development, and early cocoon production of the earthworm *Eisenia fetida*,
- 547 with particular reference to zinc. Ecotoxicology and Environmental Safety 35, 86-95.

- 548 Spurgeon, D.J., Hopkin, S.P., Jones, D.T., 1994. Effects of cadmium, copper, lead and
- 549 zinc on growth, reproduction and survival of the earthworm Eisenia fetida (Savigny):
- 550 Assessing the environmental impact of point-source metal contamination in terrestrial
- 551 ecosystems. Environmental Pollution 84, 123-130.
- 552 Sturzenbaum, S.R., Parkinson, J., Blaxter, M., Morgan, A.J., Kille, P., Georgiev, O.,
- 553 2003. The earthworm Expressed Sequence Tag project. Pedobiologia 47, 447-451.
- 554 Tong, S., von Schirnding, Y.E., Prapamontol, T., 2000. Environmental lead exposure: a
- 555 public health problem of global dimensions. Bulletin of the World Health Organization
- 556 78, 1068-1077.
- 557 Toyofuku, T., Kurzydlowski, K., Lytton, J., MacLennan, D.H., 1992. The nucleotide
- 558 binding/hinge domain plays a crucial role in determining isoform-specific Ca^{2+}
- dependence of organellar Ca⁽²⁺⁾-ATPases. Journal of Biological Chemistry 267, 1449014496.
- 561 Tsien, R.W., Hess, P., McCleskey, E.W., Rosenberg, R.L., 1987. Calcium Channels -
- 562 Mechanisms of Selectivity, Permeation, and Block. Annual Review of Biophysics and
- 563 Biomolecular Structure 16, 265-290.
- 564 Vatamaniuk, O.K., Bucher, E.A., Sundaram, M.V., Rea, P.A., 2005. CeHMT-1, a
- 565 Putative Phytochelatin Transporter, Is Required for Cadmium Tolerance in
- 566 Caenorhabditis elegans. Journal of Biological Chemistry 280, 23684.
- 567 Vilsen, B., Andersen, J.P., 1992. Deduced amino acid sequence and E1-E2 equilibrium
- of the sarcoplasmic reticulum $Ca^{(2+)}$ -ATPase of frog skeletal muscle. Comparison with
- the $Ca^{(2+)}$ -ATPase of rabbit fast twitch muscle. FEBS Letters 306, 213-218.

570	Warren, M.J., Cooper, J.B., Wood, S.P., Shoolingin-Jordan, P.M., 1998. Lead
571	poisoning, haem synthesis and 5-aminolaevulinic acid dehydratase. Trends in
572	Biochemical Sciences 23, 217-221.
573	Wimmers, L.E., Ewing, N.N., Bennett, A.B., 1992. Higher plant Ca ⁽²⁺⁾ -ATPase:
574	primary structure and regulation of mRNA abundance by salt. Proceedings of the
575	National Academy of Sciences of the United States of America 89, 9205-9209.
576	
577	
578	Figure legends
579	
580	Figure 1. Earthworm population structure superimposed on a geochemical map of the
581	Cwmystwyth Pb mine. Surface maps depicting the pH (B) and Pb (C) levels are
582	overlayed on a topographical map of the Cwmystwyth valley (D), derived from 71 and
583	97 independent measurements respectively, and generated using $SURFER^{\degree}$. The four
584	earthworm sampling sites are indicated by vertical black guide lines together with the
585	median joining networks depicting the phylogenetic structure, based upon COII
586	sequence data, of each population studied (A). The size of each haplotype group within

- 587 the network is proportional to the total number of individuals attributed to the genotype.
- 588 Mitochondrial lineage A individuals are shown as open circles whilst lineage B are
- 589 filled circles.

590

591 Figure 2. Mitochondrial and nuclear analysis of the earthworm, *L. rubellus*, population

592 structure and corresponding mitochondrial mismatch distributions. Earthworms

593 collected at four equally specially distributed sites with contrasting geo-chemical

594 properties were analysed for their mitochondrial (panel A) and nuclear (panel B) genotype. Sites included $C4_{Pb*}^{PH6}$ (blue triangles) and $C1_{Pb*}^{PH5}$ (purple diamonds), at the 595 $C2_{Pb^*}^{pH4}$ (red squares). boundary of mine, together with $C3_{Pb^{***}}^{Ph7}$ (grey circles) and 596 597 A. Median-joining network analysis based upon 440 bp sequence of the COII 598 mitochondrial gene of 119 L. rubellus individuals. The size of each haplotype group 599 within the network is proportion to the total number of individuals attributed to the 600 genotype whilst the earthworm source is indicated by fill colour. The left and right hand 601 branches of the network are denoted lineage A & B respectively. B. AFLP multi-locus 602 profiling principal component analysis showing individuals from the four sample 603 stations. Those individuals exhibiting mitochondrial lineage B genotype are circled in red whilst those attributed to lineage A are circled in grey. The clustering of $C3_{Pb}^{PH7}$ 604 605 earthworms distinct from other lineage A earthworms is indicated with a dotted grey 606 line. Hybrid individuals are shown by a lack of fill colour. C and D. Arlequin simulated 607 mitochondrial mismatch distributions, using the model of demographic expansion, of 608 lineage A (C) and lineage B (D) haplotypes respectively. The solid lines are the 609 observed mismatch distribution and the dotted line shows the distribution simulated 610 under the expansion model. E. Associated sum of squared deviation (SSD), Raggedness 611 (Rg) and p-value statistics, based on 1000 data bootstraps. 612

613 Figure 3. Metabolomic fingerprinting of earthworm chloragogenous tissue using Fourier

614 Transform Infrared spectroscopy. A. The fingerprint region of averaged infra-red

615 spectra of earthworm chloragogenous tissue collected from $C3_{Pb^{***}}^{pH7}$ (grey) and $C2_{Pb^{*}}^{pH4}$

616 (red). Individual spectra were processed by the software package $OPUS^{\circ}$). B. The main

617 difference in $C3_{Pb^{***}}^{PH7}$ and $C2_{Pb^{*}}^{PH4}$ averaged spectra (~1080cm⁻¹), corresponded to 618 phosphorus-containing functional groups, C. XLSTAT simulated dendrogram 619 illustrating the clustering of $C3_{Pb^{***}}^{PH7}$ and $C2_{Pb^{*}}^{PH4}$ earthworms according to their infra-red 620 spectral patterns (1096-1123cm⁻¹)

621

622 Figure 4. Analysis of earthworm SERCA variants. A. phylogenetic analysis of

623 genotyped individuals, based upon the cytochrome oxidase II (COII) gene, from sites

624 including the control sites $C4_{Pb*}^{pH6}$ (blue triangles) and Cl_{Pb*}^{pH5} (purple diamonds) at the

boundary of the mine and contaminated sites $C3_{Pb^{***}}^{pH7}$ (grey circles) and $C2_{Pb^{*}}^{pH4}$ (red

626 squares) alongside L. castaneus and L. eiseni (white triangles). B. Discriminatory PCR

627 illustrating the lineage-specific expression of the SERCA variants and C. PyMol

628 simulated model of SERCA. The conserved calcium binding sites are indicated in

629 yellow and amino acid differences in the two *L. rubellus* isoforms in red. The

630 phosphorylation (P) and nucleotide binding (N) domains are shown